#### Research Article

Wojciech Smułek and Maciej Jarzębski\*

# Hemp seed oil nanoemulsion with *Sapindus* saponins as a potential carrier for iron supplement and vitamin D

https://doi.org/10.1515/rams-2022-0317 received March 30, 2023; accepted April 28, 2023

**Abstract:** Vitamin D<sub>3</sub> and iron are important components of a balanced diet. Supplementing meals with these is essential to support the recovery of humankind's malnutrition. It is necessary to develop effective delivery systems to ensure the high bioavailability of these hydrophobic components. For this purpose, emulsions were prepared based on hemp seed oil and with soap nut extract (Sapindus mukorossi fruits) as a natural emulsifier. To characterize the differences in the properties of the emulsions depending on the content of the oil phase and the emulsifier, measurements were performed to determine the following parameters: the color characteristics, transparency of the samples, infrared spectrum, particle size distribution, polydispersity of the system, and the rheological properties of the emulsions. The results showed that the highest stability was observed in systems with a relatively low oil concentration, i.e., 1%. These samples also had an average particle size not exceeding 200 nm. In turn, the low oil content significantly reduced the dynamic viscosity of the emulsions. At the same time, microscopic observations indicated that the presence of an oil phase was advantageous, not only because of the possibility of providing vitamin D but also because of the high hydrophobicity of the iron particles. Therefore, the realized research made it possible to identify the optimal emulsion composition. The created system can find applications in delivering dietary supplements such as vitamin D<sub>3</sub> and iron by providing high dispersion of components and high stability.

**Keywords:** emulsion, soap nuts, saponins, iron carrier, food supplements

## 1 Introduction

One of the crucial factors influencing the effectiveness of the action of biologically active substances is their bioavailability, which corresponds with the effective dose of the compound that is successively accessing the action place, *i.e.*, receptor, co-enzyme, *etc.* [1,2]. Bioavailability is regulated and limited by biological and non-biological phenomena. Among these physical–chemical aspects, the solubility of the bioactive compound is the most limiting factor, especially for low-soluble chemicals [3].

Supplementation of fat-soluble vitamin D plays a crucial role in the process of human recovery after illness [4,5]. Moreover, it is responsible for proper growth of children and regulates critical living processes, including protection against infections [6]. Its supplementation is important as part of recovery. Unfortunately, its bioavailability is limited by its low solubility and is strongly correlated with proper digestion of the fats that are its source [7].

A similar problem is the bioavailability of iron, which is an element necessary for the proper functioning of organisms [8,9], and its deficiency is associated with anemia [10,11]. Since iron and vitamin D are key compounds for the recovery of malnourished people, with the most subjected groups of children and elderly from developing countries, it is important to create preparations that increase the bioavailability of these compounds and administer them together [12].

The starting point of our research is hemp seed oil (HSO)-based emulsions that are stabilized with saponins. Our previous studies have shown that a mixture of these ingredients provides high emulsification, leading to nanosize droplets and long stability [13,14]. It is worth mentioning that nano-size particles and droplet systems, including nanostructured lipid carrier systems, have many advantages of medical applications [15–17]. Moreover, an additional

<sup>\*</sup> Corresponding author: Maciej Jarzębski, Department of Physics and Biophysics, Poznań University of Life Sciences, 38/42 Wojska Polskiego Str., 60-637 Poznań, Poland, e-mail: maciej.jarzebski@up.poznan.pl, tel: +48 535 255 775 Wojciech Smułek: Institute of Chemical Technology and Engineering, Poznan University of Technology, 4 Berdychowo Str., 60-965 Poznań, Poland

advantage is the antibacterial properties of these emulsions that increase their shelf life. In addition, HSO is a source of unsaturated fatty acids, which are an important part of a balanced diet [18]. On the other hand, saponins are plant-derived surfactants containing hydrophobic steroids or triterpenoids linked with a hydrophilic sugar chain [19,20]. Their antioxidative and antibacterial properties make them valuable food additives [21]. Among others, *Quillaja saponaria* bark saponins (E999) are approved as foam stabilizers [22]. Previous studies by Chen *et al.* [23] showed that saponins from *Sapindus mukorossi* present high active surface properties. In their studies, the homemade saponins exhibited an expansion ratio of around 3.2, whereas that of sodium dodecyl sulfate (SDS) was equal to 7.7. However, the foam half-life increases from 322 s for SDS to 877 s for the obtained samples.

Hence, this study aims to investigate use of hempseed oil emulsions stabilized with  $S.\ mukorossi$  (soapnuts) saponins as an efficient carrier for vitamin D and iron codelivery. Based on the design of the experiment, emulsion systems with different compositions were prepared. Then, their macro- and microscopic investigations were done and infrared spectra were recorded, followed by droplet size distribution tests. Refractive index (RI) and  $L^*a^*b$  color measurements, as important consumer satisfaction factors, were also tested. Considering future processing issues, the emulsion rheology, including dynamic viscosity and shear stress, was studied. All collected results gave a broad perspective and deep insight into the properties of different emulsions and allowed the selection of the optimal composition with desired features.

## 2 Materials and methods

#### 2.1 Reagents

Cold-pressed HSO was purchased from a local market (Złoto Polskie, Kalisz, Poland). Soap nut (SN) extract

was obtained via methanol extraction in a Soxhlet apparatus according to the method described by Smułek et~al. [24]. For all experiments, distilled water without further purification was used. As an iron agent, solid particles AproFER 1000 were used (Inter JJP Sp. z o.o., Poland). Dry vitamin D<sub>3</sub> 100 CWS/AM (called vitamin D) was purchased from a regional supplier ("STANLAB" Sp. z o.o., Lublin, Poland).

#### 2.2 Sample preparation

The compositions of the emulsions hempseed formulation design (HFD) were designed using a modified and simplified Box–Behnken design for two factors: HSO content and surfactant concentration (here, nine points) based on previous studies [13,25,26]. The SN water stock solution concentration was 10 g·L $^{-1}$ . The same amount of iron and vitamin D was added to all emulsions. The compositions of the emulsions are presented in Table 1.

The emulsions were performed using a two-step homogenization procedure, previously described in the study of Jarzębski et al. [27], with some modifications. In brief, for a total volume of 25 mL of samples, the composition was placed in 50 mL plastic laboratory tubes and vortexed together for 20 s. Then, at the first step of homogenization, the components were homogenized using a hand homogenizer CAT X120 equipped with a T10 shaft for 600 s (RPM speed ca. 16,000). Directly after the first step, the samples were homogenized by ultrasonic treatment using a Sonoplus sonicator equipped with a TS109 probe (Bandelin, Berlin, Germany). Sonication parameters are as follows: time 600 s, in 5 s per 5 s action/break cycles, and amplitude 60%. Then, after cooling down at room temperature, the samples were stored at 4°C in a fridge for further experiments. Before the examinations, the samples were gently heated to room temperature (by usually placing for 1 h at room temperature).

Table 1:	Composition	of the	emulsions	samples
----------	-------------	--------	-----------	---------

Sample name	<i>F</i> 1	F2	Iron (g)	Vitamin D (g)	F1: HSO volume (mL)	F2: Surfactant SN volume (mL)	Water volume (mL)
HFD 1	0	0	0.03	0.04	0.750	0.263	23.087
HFD 2	-1	0			0.250	0.263	24.487
HFD 3	1	0			1.250	0.263	23.487
HFD 4	-1	1			0.250	0.500	24.250
HFD 5	1	1			1.250	0.500	23.250
HFD 6	0	1			0.750	0.500	23.750
HFD 7	-1	-1			0.250	0.025	24.725
HFD 8	1	-1			1.250	0.025	23.725
HFD 9	0	-1			0.750	0.025	24.225

## 2.3 Stability tests

#### 2.3.1 Visual tests

The samples were kept in plastic vials at room temperature (placed on typical laboratory shelves, where they were exposed to natural sunlight and LED light from laboratory lamps), and in a fridge at ca. 4–8°C. The condition was verified by eye observation and camera imaging (built-in camera of Samsung M11). Detailed studies were performed using a ZEISS Axio Vert.A1 microscope (Zeiss, Shanghai, China), which is an inverted microscope equipped with an Axiocam 208 color camera (Zeiss, China). Imaging was performed at different magnifications (objectives 20x, 40x, and oil 100×). Before imaging, the testing emulsion was placed into a µ-Slide VI 0.4 cuvette (ibidi GmbH, Gräfelfing, Germany) and kept for a couple of minutes to reduce droplet speed flow. Obtained images were processed using ZEN3.1 blue edition software (Zeiss, Jena, Germany).

#### 2.3.2 Dynamic light scattering (DLS) measurements

DLS was applied for hydrodynamic diameter evaluation of the prepared emulsions. Zetasizer Pro (Malvern Panalytical) with ZS XPLORER 1.0 software was used for measurements. It should be noted that the samples were studied without additional purification or dilution. For that reason, a backscattering angle of 173° was chosen. The emulsion was characterized at 25°C after conditioning for 300 s in the measuring chamber. The software was adjusted automatically for latex standards, and each sample was measured five times (representative curves corresponding to the average values were presented).

#### 2.3.3 Centrifuge stability tests

A two-step centrifugation process for the emulsion stability verification was chosen. Samples (1.5 mL) were placed in 2 mL Eppendorf test tubes and centrifuged. First, the centrifugation condition was adjusted at 5,000 RPM for 10 min. Then, the samples were visually observed and centrifuged for another 10 min at 10,000 RPM. Stability was evaluated by observing oil phase separation.

## 2.4 Spectrophotometric analysis

UV-vis spectra of the emulsion were collected using a UV/Vis UV-3100PC spectrometer in the range of 190-1,100 nm. Further studies were done with Spectrum Two FT-IR spectrometer equipped using a Universal ATR with a diamond crystal (PerkinElmer, Waltham, MA, USA) to determine FT-IR spectra in the range of 500–4,000 cm<sup>-1</sup>. For each sample, the measurements were repeated three times.

#### 2.5 Viscosity determination

ViscoQC 300 (Anton Paar Gmbh, Graz, Austria), a programmable rotational viscometer, was used to determine rheological properties of the emulsions. The tests were performed at room temperature without additional adjustments. The liquid emulsion samples were placed into a "double-gap" C-DG26 measuring cup with a B-DG 26 measuring bob. The speed of the spindle ranged from 2 to 250 RPM. Each test was performed in triplicate.

## 2.6 Turbidity tests

For the emulsion turbidity evaluation, a Eutech™ TN-100 turbidimeter (Thermo Fisher Scientific) was used. Before the measurements, the turbidimeter was adjusted using turbidity standards: 0.02, 20.0, 100, and 800 NTU. Then liquid samples were placed in dedicated glass vials with cups. All measurements were repeated five times, and the average values were calculated.

## 2.7 pH determination

A portable S2-Food-Kit Seven2Go pH meter (Mettler Toledo) equipped with an InLab Solids Go-ISM electrode was used for pH evaluation. The average values of five repetitions were calculated.

#### 2.8 Color analysis

An NH310 portable spectrophotometer (Shenzhen ThreeNH Technology Co., Ltd., Shiyan, China) equipped with internal software was used. Two milliliters of the sample were inserted into a transparent plastic cuvette and placed into a dedicated measurement chamber. The color tests were repeated ten times, and the average values with SD were recorded. The  $\Delta E^*ab$  was calculated using the following formula:

$$\Delta E_{Lab}^* = \sqrt{(\Delta L^*)^2 + (\Delta a^*)^2 + (\Delta b^*)^2}$$

where  $\Delta L^{\star}$ ,  $\Delta a^{\star}$ , and  $\Delta b^{\star}$  are the differences between values of  $L^*$ ,  $a^*$ , and  $b^*$  between the average of the measurements of each two comparing sample.

#### 2.9 RI

A portable PAL-RI optical electronic refractometer (ATANGO CO., LTD, Tokyo, Japan) was used to determine RI. The RI of the emulsion was collected at room temperature. For all samples, the measurements were repeated ten times and the mean value with SD was calculated.

#### 2.10 Statistical analysis

All experiments carried out as part of the study were performed in triplicate minimally (if more, it is stated separately). Analysis of variance (ANOVA) with a significance level of p < 0.05 was used to assess the statistical significance of the results.

## 3 Results and discussion

## 3.1 Macroscopic properties of emulsions

Previous studies by Fathordoobady *et al.* [26] proved that HSO and HSO-based emulsions can be considered potentially active agent carriers. Iron supplements, in solid forms, are typically stored in oil dispersion form or gelatin capsules. For oral admission, especially for children and infants, it is beneficial to design supplements in liquid form. The AproFER 1000 iron diet supplements used here were studied previously by Grzechulska-Damszel *et al.* [28] due to their microbial and magnetic properties and chemical compositions.

The prepared emulsion systems with the compositions described in Table 1 are presented in Figure 1a. It should be noted that some of the systems, such as HFD1 and HFD5, showed relatively rapid phase separation. It was detected during the turbidity test (described in the other part of the text). Then after a couple of hours, almost full separation was observed in some samples. In contrast, HFD2 and HFD 4 emulsions showed high homogeneity, which was also noticed after centrifugation (Figure 1b). Slight phase separation was observed in HFD7, although it was also a very stable system. At this observation stage, it could be concluded that a relatively low level of HSO was advantageous for maintaining homogeneity. At its higher concentrations, phase separation was observed. Additionally, the higher the SN concentration, the more homogeneous the emulsion was. In almost all of the samples, sediment deposition on the

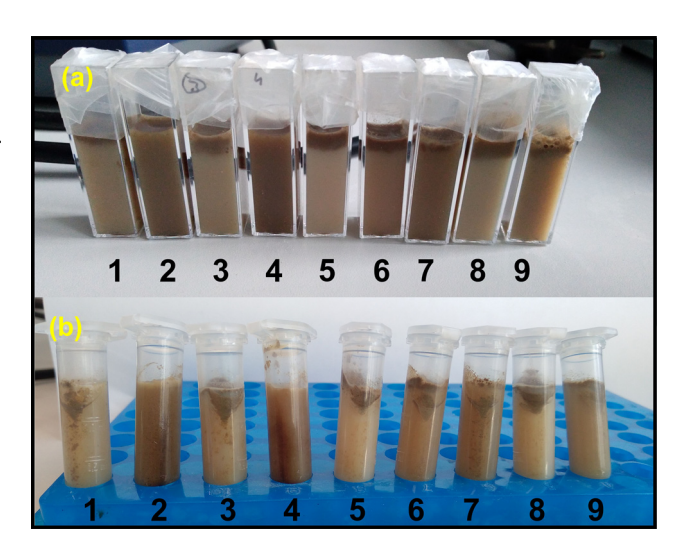


Figure 1: HFD emulsions: (a) after preparation, (b) after centrifugation (numbers 1–9 correspond to HFD 1–9).

walls was observed. However, the best volume distribution of solid iron particles can be seen in samples HFD2, HFD4, and HFD7 (Figure 1). The presence of the iron formulation resulted in a brownish color of the emulsion. Most of the iron supplements are concentrated in the oil phase. This confirmed the original hypothesis, assuming that the emulsion system could be a good solution to increase its dispersion in the liquid. Considering that the systems studied are going/intended to be used in the food industry or as delivery agents for dietary supplements, issues related to their appearance are important to ensure the attractiveness of the products to consumers. For oral admission, food properties such as taste and color should be modified by artificial agents.

Moreover, the RI (Figure 2a) and the color of the samples were examined (Table 2). The RI of emulsions ranged from 1.3345 to 1.3377, and it could be noticed that its increase is positively correlated with an increase in HSO concentration. For food products and supplements, specially dedicated to kids, color plays a crucial role as well as taste [29]. Color dimensions in the  $L^*a^*b$  space indicated that HSO concentration results in an L factor increase and a factor decrease. No significant effect on the b factor was observed. No impact of SN concentration on RI or color was observed.

Furthermore, the pH of emulsions was studied (Figure 2b). The pH value varied from 5.60 and 6.05. However, no statistically significant differences in the acidity of the samples were observed. As mentioned, the color of a multiphase system can have a significant impact on its evaluation by consumers, and appropriate modification can increase the attractiveness of the product [30]. Since the content of iron particles was the same in all samples,

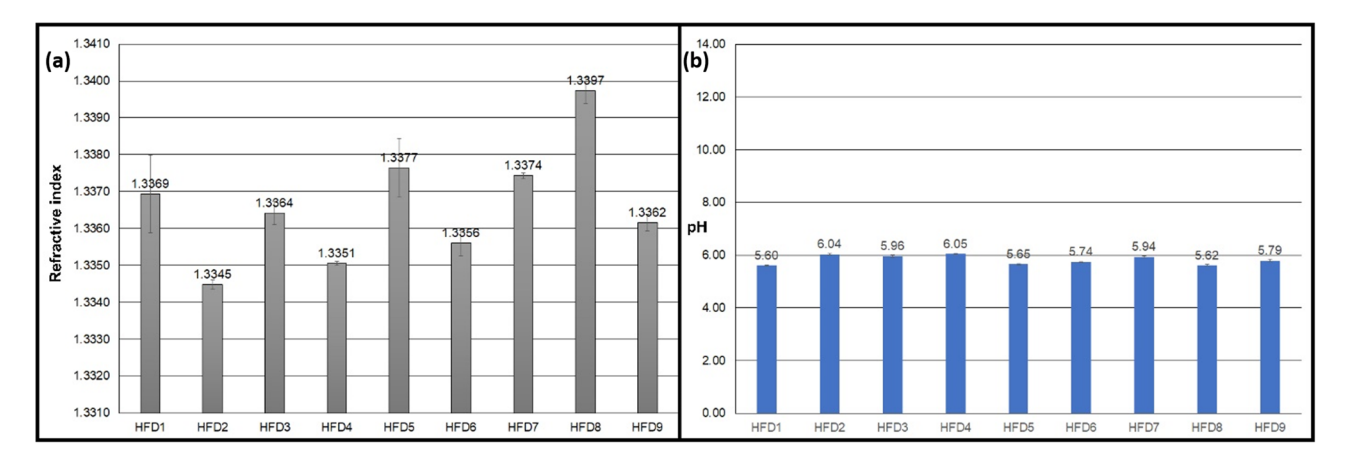


Figure 2: Emulsions properties: (a) RI (left side), (b) pH values.

the observed changes in color and RI values are a consequence of how the iron particles and emulsion droplets are dispersed. More homogeneous samples were darker with uniform color. However, the influence of the surfactant should also be considered. As noted by Chung *et al.* [31], saponins, like any surfactant, can change the path of light on their micelles to some extent. Additionally, from their chemical nature, they can selectively absorb particular electromagnetic radiation bands.

The next stage of the study involved recording infrared spectra for the emulsion samples and the main emulsion components (HSO and SN) (Figure 3). The spectra obtained for the emulsion show strong and broad signals with a maximum at 3,300 cm<sup>-1</sup> coming from OH groups present in both water, which is the continuous phase, and SN. The HSO and SN spectra show a group of signals between 3,100 and 2,800 cm<sup>-1</sup> representing stretching vibrations of C–H bonds. However, only the HSO spectrum shows signals above 3,000 cm<sup>-1</sup>, which corresponds to C–H bonds in the vicinity of unsaturated carbon–carbon bonds. These bonds are characteristic for unsaturated fatty acids, whose

significant amounts are present in HSO. Also, from these acids, or more precisely from the bonds of the carbonyl group, comes a very intense signal at 1,750 cm<sup>-1</sup>. A similar signal, although weak and shifted toward smaller wave numbers, is seen in the SN spectrum. It also corresponds to C=O groups but is present in other types of molecules, such as steroids, which are components of saponins. Another intense signal in the SN spectrum is the one with a maximum at 1,650 cm<sup>-1</sup>, which most likely corresponds to another C=O group present in saponins.

At lower wavenumbers, only signals from deformation vibrations in the C–H bonds and stretching of the C–O bonds are visible. These signals are only observed for SN and HSO samples. It was important for our study to indicate that signals from HSO and saponins are also visible in the emulsion spectra – they are most clearly visible in the spectrum of HFD9 and weakly but still noticeably present in the spectrum of samples HFD8 and HFD4. In the other samples, only signals from bonds in water and a signal at 1,650 cm<sup>-1</sup> such as in SN are visible. Interestingly, this relative intensity of signals in

**Table 2:** Color analysis  $(L^*-a^*-b^*)$  and lightness; relative intensity marks in Classification section: + low, ++ medium, +++ intensive

Sample name		Color	Classification			
	L*	a*	b*	Lightness	Green	Blue
HFD 1	40.97 ± 0.02	1.09 ± 0.04	2.75 ± 0.04	Dark++	++	++
HFD 2	$40.81 \pm 0.01$	$1.34 \pm 0.04$	$2.34 \pm 0.04$	Dark++	++	++
HFD 3	$48.18 \pm 0.05$	$1.03 \pm 0.02$	$4.38 \pm 0.03$	Light+	++	+++
HFD 4	$39.21 \pm 0.01$	$1.54 \pm 0.03$	$2.32 \pm 0.04$	Dark++	+++	++
HFD 5	$49.45 \pm 0.69$	$0.16 \pm 015$	$2.96 \pm 0.23$	Light+	+	++
HFD 6	$42.41 \pm 0.06$	$1.18 \pm 0.06$	$2.47 \pm 0.13$	Dark++	++	++
HFD 7	$41.83 \pm 0.02$	$0.97 \pm 0.04$	$2.62 \pm 0.04$	Dark++	++	++
HFD 8	44.50 ± 1.89	$1.09 \pm 0.26$	$2.92 \pm 0.20$	Light+	++	++
HFD 9	$45.98 \pm 0.06$	$1.17\pm0.04$	$3.67 \pm 0.04$	Light+	++	++

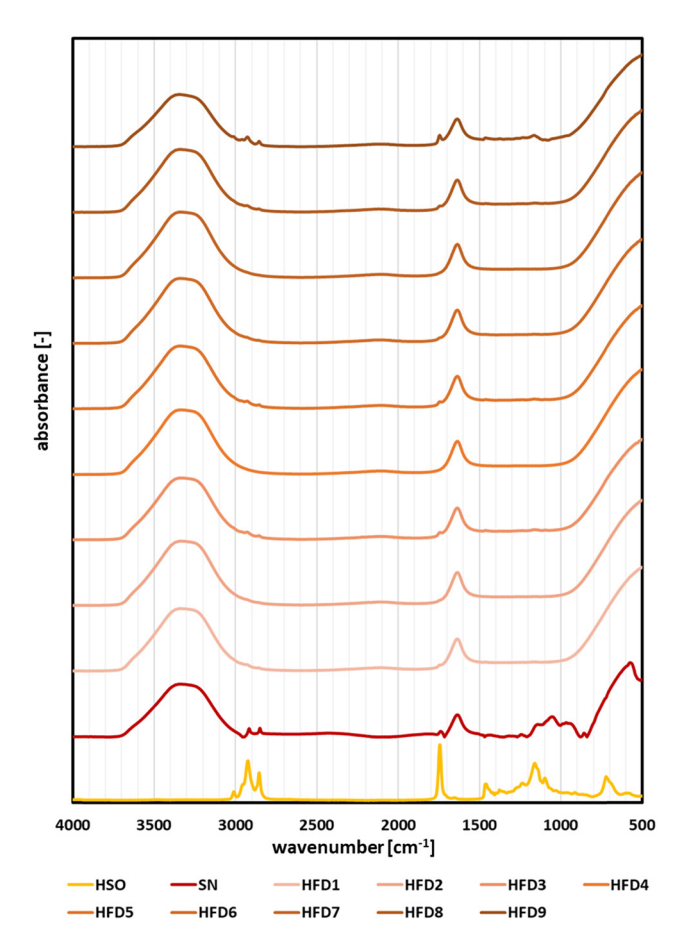


Figure 3: Infrared spectra (ATR-FTIR) of tested emulsions (HFD 1-9), SN extract, and hempseed oil (HSO).

the samples is not directly correlated with the percentage of components. For example, the highest content of HSO was present in samples HFD3, HFD5, and HFD8, within which signals from HSO are not seen as intensely. So, the dispersion/agglomeration factor of the oil phase of the emulsion may be relevant here, and this is a factor that projected the intensity of the signals. Nevertheless, assessing whether ATR-FTIR spectra of emulsions can be a tool to evaluate the quality of emulsion dispersion requires further analysis.

## 3.2 Emulsion particle size analysis

Further investigations focused on the properties of the emulsions with regard to their droplet size and uniformity. Images of the emulsions recorded using an inverted optical microscope are presented in Figure 4. A comparison of the individual samples shows differences in the color and permeability of the samples. It also confirms the agglomeration of iron particles in the organic phase,

although primarily in the form of aggregates at the oil—water interface. Relatively larger HSO droplets are seen for samples HFD3, HFD6, and HFD9. Additionally, it should be noted that the tested systems show an average level of homogeneity, as the images show structures of different shapes and sizes, indicating that the emulsions combine the features of iron particle suspension, in both water and oil phases, and oil-in-water emulsions.

Microscopic observations correspond to the measurements of particle size distribution in the samples, for which the most important results are summarized in Table 3. Average particle/droplet size (z-Ave) ranges between 172 nm (for HFD7) and 377 nm (for HFD3); however, the majority of samples have z-Ave values of approximately 200 nm or lower. The only exceptions were HFD3 and HFD6 samples. The samples were characterized by a relatively low polydispersity index (PDI), not exceeding 0.509 (HFD3). It can be seen that an increase in concentration of both HSO and SN caused a PDI increase. Moreover, it should be noted that we did not dilute the samples to prevent the destabilization of the emulsions. This way of presentation is more beneficial, due to the recognition of the impact of used stabilizers, here SNs. In this study, the term particle is more appropriate due to emulsion composition. DLS is one of the "blind" methods that does not allow recognizing solid particles from droplets, etc. Furthermore, the results proved that the DLS results (Figure 5) should be compared with some visual techniques [32].

Saponins are well recognized as effective emulsifiers allowing them to obtain nanoemulsions [33]. Saponins from Q. saponaria made it possible to obtain emulsions of medium-chain triglycerides with droplet sizes of about 200 nm, a result comparable to those obtained with Tween80 [34]. Also, studies by Sotomayor-Gerding et al. [35] showed that saponins from Q. saponaria provide an emulsifier comparable to Tween20. However, saponins from S. mukorossi have not been widely studied to date, especially in systems with natural oils. A few examples include the research of Gundewadi et al. [36], who emulsified basil oil and obtained nanoemulsions with particle sizes of 200 nm and below using S. mukorossi extract. In addition, Tsibranska et al. [37] noted that saponins from various sources show strong adsorption on the surface of dispersed oil droplets, leading to stable deformations of the emulsion droplets. In the case described in this article, when iron particles are still present, this effect may be even stronger, which would be confirmed by the measured values of the PDI and homogeneity of structures on the micrometer scale observed microscopically.

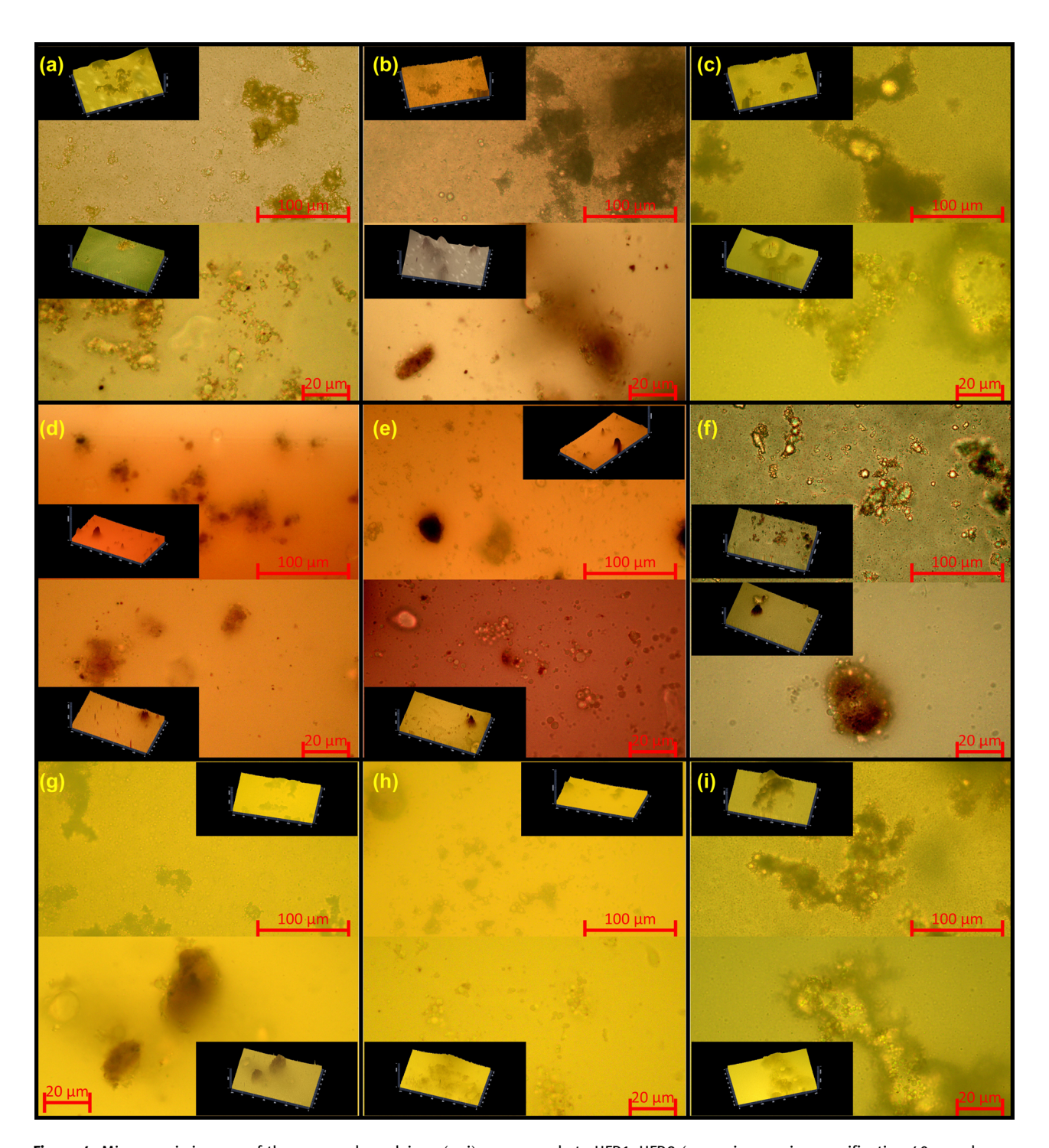


Figure 4: Microscopic images of the prepared emulsions (a-i) corresponds to HFD1-HFD9 (upper images in magnification  $40\times$ , under images in magnification  $100\times$ ). Inserted images within 2.5D.

## 3.3 Rheological properties of emulsions

The final stage of the research involved studying the rheological properties of the obtained emulsions. Measurement results of dynamic viscosity and shear stress are shown in Figures 6 and 7. The collected data indicate a strong

dependence of these parameters on the composition of the emulsion. The highest dynamic viscosity values, exceeding 3.0 mPa·s, were found for samples HFD3, HFD5, and HFD8. The lowest dynamic viscosity of 1.48 mPa·s was measured for samples HFD2 and HFD4. The trends for shear stress are proportional to those for dynamic viscosity; *i.e.*, the highest values

**Table 3:** Droplet average size (z-ave), PDI, main peak maximum, turbidity; different small letters indicate groups that differ significantly at p < 0.05

Sample name	z-ave (nm)	PDI (—)	Main peak maximum (intensity) (nm)	Main peak maximum (number) (nm)	Turbidity
HFD 1	175 ± 2 <sup>a</sup>	$0.281 \pm 0.029^a$	224 ± 10 <sup>a</sup>	55 ± 19 <sup>ab</sup>	141 ± 4* <sup>a</sup>
HFD 2	$193 \pm 5^{b}$	$0.270 \pm 0.031^a$	235 ± 11 <sup>a</sup>	85 ± 27 <sup>ab</sup>	$184 \pm 1^{b}$
HFD 3	$377 \pm 39^{c}$	$0.509 \pm 0.012 b$	299 ± 16 <sup>b</sup>	$71 \pm 62^{ab}$	$60 \pm 4*^{c}$
HFD 4	$192 \pm 6^{b}$	$0.265 \pm 0.010^a$	253 ± 36 <sup>abc</sup>	81 ± 29 <sup>ab</sup>	179 ± 7 <sup>b</sup>
HFD 5	$206 \pm 2^b$	$0.373 \pm 0.015^{c}$	259 ± 13 <sup>c</sup>	39 ± 11 <sup>a</sup>	137 ± 4* <sup>a</sup>
HFD 6	$277 \pm 19^{d}$	$0.491 \pm 0.040^{b}$	296 ± 16 <sup>b</sup>	67 ± 15 <sup>ab</sup>	$241 \pm 19^{*d}$
HFD 7	$172 \pm 2^a$	$0.243 \pm 0.011^a$	207 ± 22 <sup>ae</sup>	94 ± 20 <sup>ac</sup>	$281\pm20^d$
HFD 8	$173 \pm 2^{a}$	$0.256 \pm 0.005^a$	213 ± 5 <sup>ae</sup>	65 ± 33 <sup>ab</sup>	75 ± 5* <sup>e</sup>
HFD 9	$201\pm5^b$	$0.329 \pm 0.033^{c}$	$242 \pm 10^{abc}$	43 ± 11 <sup>ab</sup>	$158\pm18^{ab}$

<sup>\*</sup>Fast phase separation. Detailed comments are given in the text.

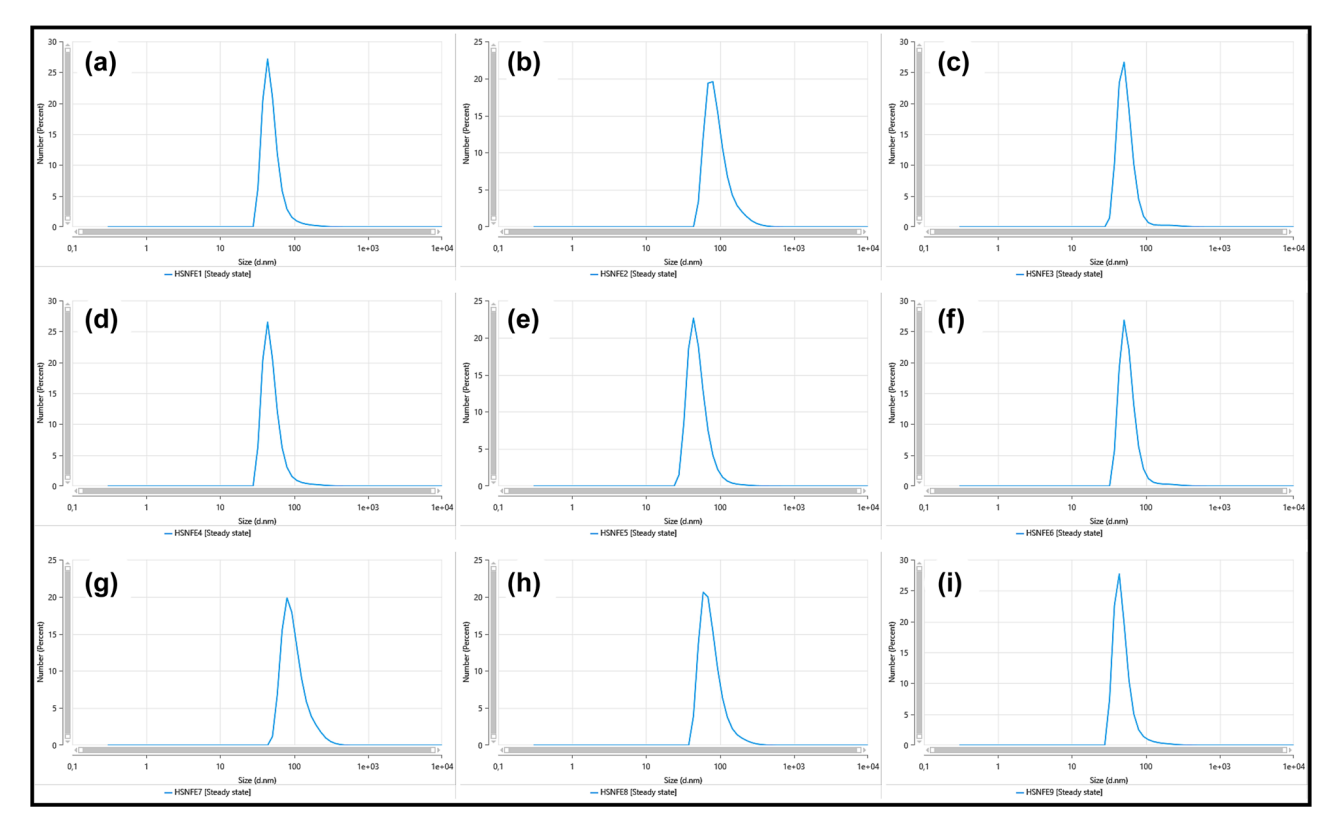


Figure 5: Particle size distribution by the number obtained by DLS (a-i) sample HFD1-9, respectively.

were recorded for HFD8 and HFD5 (0.1940 and 0.1713  $\rm N\cdot m^{-2}$ ), respectively, and the lowest were recorded for HFD2 and HFD4 (0.0763  $\rm N\cdot m^{-2}$ ). The shapes of the dynamic viscosity vs rotation rate and shear stress vs shear rate curves are analogous for all samples, and at relatively low values, they overlap with each other to diverge at higher rates (Figure 7, for selected samples). The curves in Figure 7b show that the tested emulsions have the character of a Newtonian fluid with slight shear-thinning fluid properties, which noticeably change at relatively high values of shear stress (above 150 s<sup>-1</sup>).

When considering the rheological properties of the studied systems, one should keep in mind the complex nature of the created colloids, in which both oil phase droplets and iron particles are dispersed. Rheological tests performed by Rezler showed that the concentration of each compound of the emulsion impacted the organization of its structure [38]. The iron particles can further stabilize emulsions but at the same time modify their rheological properties, as observed for Pickering-type emulsions [39,40]. The rheological properties of

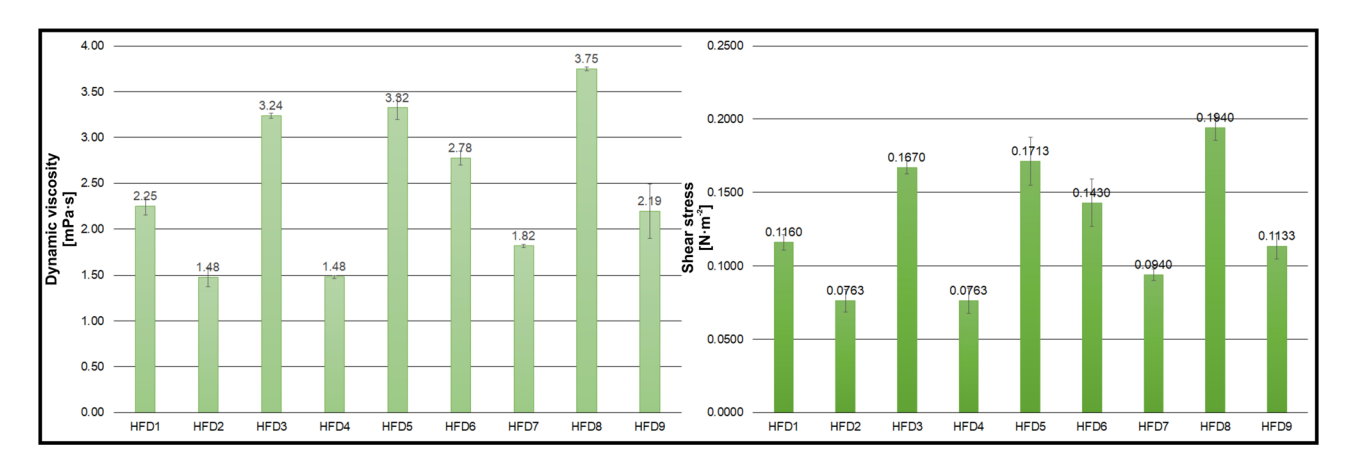


Figure 6: Dynamic viscosity (left side), shear stress (right side) registered at 40 RPM.

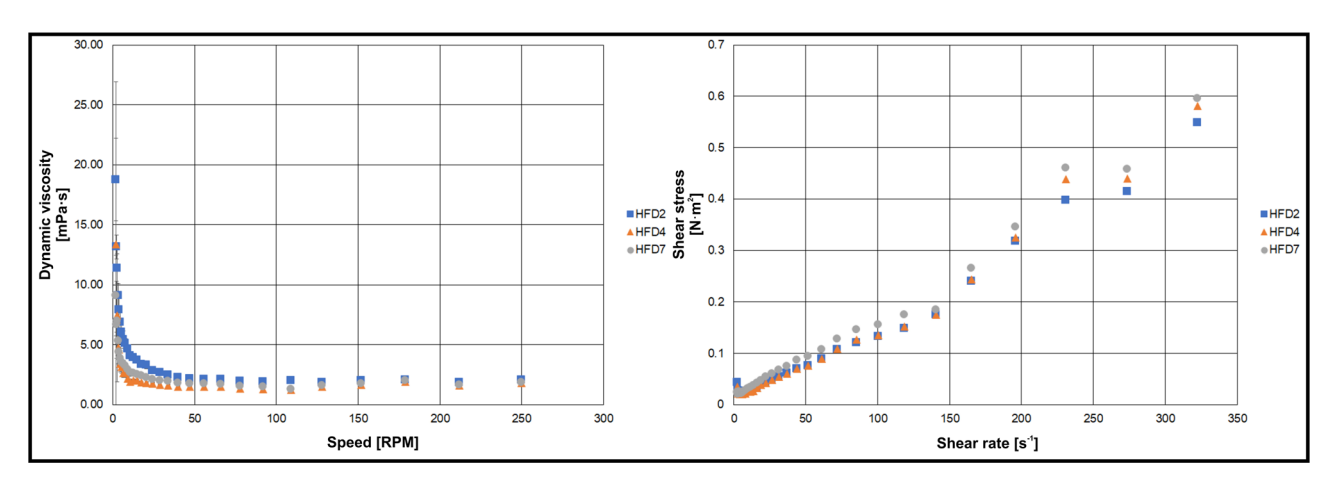


Figure 7: Dynamic viscosity versus speed (left side), shear stress versus shear rate (right side) for HFD2, HFD4, and HFD7 samples.

emulsions containing rhamnolipids and saponins from *Q. saponaria* were studied by Li *et al.* [41]. They found that emulsions stabilized by these natural surfactants presented shear-thinning behaviors, corresponding to the results presented in this paper.

# 4 Conclusions

To evaluate the possible use of SNs as a natural stabilizer for iron supplements, nine different emulsion compositions with vitamin  $D_3$  were performed. The emulsions were most stable and homogeneous at 1% HSO content. An increase in HSO content promoted phase separation, increased the RI, and impacted on color change. Dynamic viscosity was higher at higher HSO contents. It should be highlighted that the SN extract can be successfully applied as an emulsion stabilizer. Furthermore, the two-

step preparation process increases emulsion stability due to reducing emulsion droplet size.

The results made it possible to broadly characterize emulsions containing vitamin  $D_3$  and iron both from the perspective of physicochemical properties and characteristics necessary for consumer appeal (e.g., color) and processing parameters (dynamic viscosity). The HFD4 emulsion containing 1% HSO and 0.2% SN can be identified as the optimal system. At the same time, the properties of the system show that it can become an effective delivery system for compounds that are dietary supplements.

**Acknowledgments:** The authors thank Inter JJP Sp. z o.o., Poznań, Poland, for the AproFER 1000 samples used in this research.

**Funding information:** This study was financially supported with grant MINIATURA 2021/05/X/NZ9/00384 from National Science Centre Poland.

**Author contributions:** Conceptualization, methodology, formal analysis, investigation, resources, data curation, writing - original draft, review and editing: Wojciech Smułek and Maciej Jarzębski. Validation: Wojciech Smułek. Supervision, project administration, funding acquisition: Maciej Jarzębski. All authors have accepted responsibility for the entire content of this manuscript and approved its submission.

**Conflict of interest:** Maciej Jarzębski, who is the coauthor of this article, is a current Editorial Board member of *Reviews on Advanced Materials Science*. This fact did not affect the peer-review process. The authors declare no other conflict of interest.

## References

- [1] Rein, M. J., M. Renouf, C. Cruz-Hernandez, L. Actis-Goretta, S. K. Thakkar, and M. da Silva Pinto. Bioavailability of bioactive food compounds: A challenging journey to bioefficacy: Bioavailability of bioactive food compounds. *British Journal of Clinical Pharmacology*, Vol. 75, No. 3, 2013 Mar, pp. 588–602.
- [2] Neilson, A. P., K. M. Goodrich, and M. G. Ferruzzi. Bioavailability and metabolism of bioactive compounds from foods. *Nutrition in the prevention and treatment of disease* [*Internet*], Elsevier, Amsterdam, 2017, pp. 301–319. [cited 2023 Mar 27]. https://linkinghub.elsevier.com/retrieve/pii/ B9780128029282000151.
- [3] Smułek, W. and E. Kaczorek. Factors influencing the bioavailability of organic molecules to bacterial cells—A mini-review. *Molecules*, Vol. 27, No. 19, 2022 Oct 4, id. 6579.
- [4] Marek, K., N. Cichoń, J. Saluk-Bijak, M. Bijak, and E. Miller. The role of vitamin D in stroke prevention and the effects of its supplementation for post-stroke rehabilitation: A narrative review. *Nutrients*, Vol. 14, No. 13, 2022 Jul 4, id. 2761.
- [5] Teymoori-Rad, M., F. Shokri, V. Salimi, and S. M. Marashi. The interplay between vitamin D and viral infections. *Reviews* in *Medical Virology*, Vol. 29, No. 2, 2019 Mar, id. e2032.
- [6] Taha, R., S. Abureesh, S. Alghamdi, R. Y. Hassan, M. M. Cheikh, R. A. Bagabir, et al. The relationship between vitamin D and infections including COVID-19: Any hopes? *International Journal of General Medicine*, Vol. 14, 2021 Jul, pp. 3849–3870.
- [7] Šimoliūnas, E., I. Rinkūnaitė, Ž. Bukelskienė, and V. Bukelskienė. Bioavailability of different vitamin D oral supplements in laboratory animal model. *Medicina*, Vol. 55, No. 6, 2019 Jun 10, id. 265.
- [8] Zielińska-Dawidziak, M. Plant ferritin—A source of iron to prevent its deficiency. *Nutrients*, Vol. 7, No. 2, 2015 Feb 12, pp. 1184–1201.
- [9] Zielińska-Dawidziak, M., I. Hertig, H. Staniek, D. Piasecka-Kwiatkowska, and K. W. Nowak. Effect of iron status in rats on the absorption of metal ions from plant ferritin. *Plant Foods for Human Nutrition*, Vol. 69, No. 2, 2014 Jun, pp. 101–107.

- [10] Kangas, S. T., C. Salpéteur, V. Nikièma, L. Talley, A. Briend, C. Ritz, et al. Vitamin A and iron status of children before and after treatment of uncomplicated severe acute malnutrition. Clinical Nutrition, Vol. 39, No. 11, 2020 Nov, pp. 3512–3519.
- [11] Stoffel, N. U., H. K. von Siebenthal, D. Moretti, and M. B. Zimmermann. Oral iron supplementation in iron-deficient women: How much and how often? *Molecular Aspects of Medicine*, Vol. 75, 2020 Oct, id. 100865.
- [12] Merker, M., A. Amsler, R. Pereira, R. Bolliger, P. Tribolet, N. Braun, et al. Vitamin D deficiency is highly prevalent in malnourished inpatients and associated with higher mortality: A prospective cohort study. *Medicine*, Vol. 98, No. 48, 2019 Nov, id. e18113.
- [13] Jarzębski, M., P. Siejak, W. Smułek, F. Fathordoobady, Y. Guo, J. Pawlicz, et al. Plant extracts containing saponins affects the stability and biological activity of hempseed oil emulsion system. *Molecules*, Vol. 25, No. 11, 2020 Jun 10, id. 2696.
- [14] Martel-Estrada, S. A., A. I. Morales-Cardona, C. L. Vargas-Requena, J. A. Rubio-Lara, C. A. Martínez-Pérez, and F. Jimenez-Vega. Delivery systems in nanocosmeceuticals. *Reviews on Advanced Materials Science*, Vol. 61, No. 1, 2022 Dec 27, pp. 901–930.
- [15] Abdellatif, A. A. H., H. A. Mohammed, R. A. Khan, V. Singh, A. Bouazzaoui, M. Yusuf, et al. Nano-scale delivery: A comprehensive review of nano-structured devices, preparative techniques, site-specificity designs, biomedical applications, commercial products, and references to safety, cellular uptake, and organ toxicity. *Nanotechnology Reviews*, Vol. 10, No. 1, 2021 Oct 21, pp. 1493–1559.
- [16] Javed, S., B. Mangla, Y. Almoshari, M. H. Sultan, and W. Ahsan. Nanostructured lipid carrier system: A compendium of their formulation development approaches, optimization strategies by quality by design, and recent applications in drug delivery. *Nanotechnology Reviews*, Vol. 11, No. 1, 2022 Apr 22, pp. 1744–1777.
- [17] Maamoun, W., M. I. Badawi, A. A. Aly, and Y. Khedr. Nanoparticles in enhancing microwave imaging and microwave Hyperthermia effect for liver cancer treatment. *Reviews on Advanced Materials Science*, Vol. 60, No. 1, 2021 Jan 1, pp. 223–236.
- [18] Vodolazska, D. and C. Lauridsen. Effects of dietary hemp seed oil to sows on fatty acid profiles, nutritional and immune status of piglets. *Journal of Animal Science and Biotechnology*, Vol. 11, No. 1, 2020 Dec, id. 28.
- [19] Góral, I. and K. Wojciechowski. Surface activity and foaming properties of saponin-rich plants extracts. *Advances in Colloid and Interface Science*, Vol. 279, 2020 May, id. 102145.
- [20] Mondal, M. H., S. Malik, A. Garain, S. Mandal, and B. Saha. Extraction of natural surfactant saponin from soapnut (Sapindus mukorossi) and its utilization in the remediation of hexavalent chromium from contaminated water. *Tenside, Surfactants, Detergents*, Vol. 54, No. 6, 2017 Nov 15, pp. 519-529.
- [21] Kozińska, N., K. Tokarska, M. Chudy, and K. Wojciechowski. Cytotoxicity of quillaja saponaria saponins towards lung cells is higher for cholesterol-rich cells. *Biophysica*, Vol. 1, No. 2, 2021 Apr 6, pp. 126–136.
- [22] EFSA Panel on Food Additives and Flavourings (FAF), M. Younes, G. Aquilina, L. Castle, K. Engel, P. Fowler, et al. Reevaluation of Quillaia extract (E 999) as a food additive and

- safety of the proposed extension of use. *EFS2* [*Internet*], Vol. 17, No. 3, 2019 Mar. [cited 2023 Mar 27] https://data.europa.eu/doi/10.2903/j.efsa.2019.5622.
- [23] Chen, C., R. Li, D. Li, F. Shen, G. Xiao, and J. Zhou. Extraction and purification of saponins from *Sapindus mukorossi*. New Journal of Chemistry, Vol. 45, No. 2, 2021, pp. 952-960.
- [24] Smułek, W., A. Zdarta, M. Łuczak, P. Krawczyk, T. Jesionowski, and E. Kaczorek. Sapindus saponins' impact on hydrocarbon biodegradation by bacteria strains after short- and long-term contact with pollutant. *Colloids and Surfaces B: Biointerfaces*, Vol. 142, 2016 Jun, pp. 207–213.
- [25] Pratap-Singh, A., Y. Guo, S. Lara Ochoa, F. Fathordoobady, and A. Singh. Optimal ultrasonication process time remains constant for a specific nanoemulsion size reduction system. *Scientific Reports*, Vol. 11, No. 1, 2021 Apr 29, id. 9241.
- [26] Fathordoobady, F., N. Sannikova, Y. Guo, A. Singh, D. D. Kitts, and A. Pratap-Singh. Comparing microfluidics and ultrasonication as formulation methods for developing hempseed oil nanoemulsions for oral delivery applications. *Scientific Reports*, Vol. 11, No. 1, 2021 Jan 8, id. 72.
- [27] Jarzębski, M., W. Smułek, P. Siejak, R. Rezler, J. Pawlicz, T. Trzeciak, et al. Aesculus hippocastanum L. as a stabilizer in hemp seed oil nanoemulsions for potential biomedical and food applications. *International Journal of Molecular Sciences*, Vol. 22, No. 2, 2021 Jan 17, id. 887.
- [28] Grzechulska-Damszel, J., A. Markowska-Szczupak, G. Zolnierkiewicz, J. Typek, N. Guskos, and A. W. Morawski. On the characteristic and stability of iron diet supplements. *Polish Journal* of Chemical Technology, Vol. 21, No. 3, 2019 Sep 1, pp. 60–67.
- [29] Sahu, D., D. Bharti, D. Kim, P. Sarkar, and K. Pal. Variations in microstructural and physicochemical properties of candelilla wax/rice bran oil-derived oleogels using sunflower lecithin and soya lecithin. *Gels*, Vol. 7, No. 4, 2021 Nov 22, id. 226.
- [30] Chung, C., A. Sher, P. Rousset, and D. J. McClements. Use of natural emulsifiers in model coffee creamers: Physical properties of Quillaja saponin-stabilized emulsions. *Food Hydrocolloids*, Vol. 67, 2017 Jun, pp. 111–119.
- [31] Chung, C., A. Sher, P. Rousset, E. A. Decker, and D. J. McClements. Formulation of food emulsions using natural emulsifiers: Utilization of Quillaja saponin and soy lecithin to fabricate liquid coffee whiteners. *Journal of Food Engineering*, Vol. 209, 2017 Sep, pp. 1–11.

- [32] Jarzębski, M., B. Bellich, T. Białopiotrowicz, T. Śliwa, J. Kościński, and A. Cesàro. Particle tracking analysis in food and hydrocolloids investigations. *Food Hydrocolloids*, Vol. 68, 2017 Jul, pp. 90–101.
- [33] Schreiner, T. B., M. M. Dias, M. F. Barreiro, and S. P. Pinho. Saponins as natural emulsifiers for nanoemulsions. *Journal of Agricultural and Food Chemistry*, Vol. 70, No. 22, 2022 Jun 8, pp. 6573-6590.
- [34] Yang, Y., M. E. Leser, A. A. Sher, and D. J. McClements. Formation and stability of emulsions using a natural small molecule surfactant: Quillaja saponin (Q-Naturale®). *Food Hydrocolloids*, Vol. 30, No. 2, 2013 Mar, pp. 589–596.
- [35] Sotomayor-Gerding, D., E. Morales, and M. Rubilar. Comparison between quinoa and quillaja saponins in the formation, stability and digestibility of astaxanthin-canola oil emulsions. *Colloids and Interfaces*, Vol. 6, No. 3, 2022 Aug 28, id. 43.
- [36] Gundewadi, G., D. J. Sarkar, S. G. Rudra, and D. Singh. Preparation of basil oil nanoemulsion using Sapindus mukorossi pericarp extract: Physico-chemical properties and antifungal activity against food spoilage pathogens. *Industrial Crops and Products*, Vol. 125, 2018 Dec, pp. 95–104.
- [37] Tsibranska, S., S. Tcholakova, K. Golemanov, N. Denkov, E. Pelan, and S. D. Stoyanov. Role of interfacial elasticity for the rheological properties of saponin-stabilized emulsions. *Journal of Colloid and Interface Science*, Vol. 564, 2020 Mar, pp. 264-275.
- [38] Rezler, R. The role of starch in shaping the rheo-mechanical properties of fat-in-water emulsions. *Polysaccharides*, Vol. 3, No. 4, 2022 Dec 5, pp. 804–817.
- [39] Fu, L., Q. Ma, K. Liao, J. An, J. Bai, and Y. He. Application of pickering emulsion in oil drilling and production. *Nanotechnology Reviews*, Vol. 11, No. 1, 2021 Dec 3, pp. 26–39.
- [40] Wong, S. K., L. E. Low, J. Supramaniam, S. Manickam, T. W. Wong, C. H. Pang, et al. Physical stability and rheological behavior of Pickering emulsions stabilized by protein-poly-saccharide hybrid nanoconjugates. *Nanotechnology Reviews*, Vol. 10, No. 1, 2021 Sep 27, pp. 1293-1305.
- [41] Li, Z., L. Dai, D. Wang, L. Mao, and Y. Gao. Stabilization and rheology of concentrated emulsions using the natural emulsifiers quillaja saponins and rhamnolipids. *Journal of Agricultural and Food Chemistry*, Vol. 66, No. 15, 2018 Apr 18, pp. 3922–3929.